Available online at www.sciencedirect.com
ScienceDirect
Trans. Nonferrous Met. Soc. China 25(2015) 2147−2155
Transactions of Nonferrous Metals Society of China
www.tnmsc.cn

Effects of heat input in friction stir welding on microstructure and mechanical properties of AA3003-H18 plates

B. ABNAR, M. KAZEMINEZHAD, A. H. KOKABI

Department of Materials Science and Engineering, Sharif University of Technology, Azadi Avenue, Tehran, Iran

Received 21 August 2014; accepted 5 May 2015

Abstract: The non-heat-treatable AA3003-H18 plates were joined by friction stir welding (FSW) to achieve a proper joint by optimizing the welding parameters. For this purpose, the effects of heat input on microstructure and mechanical properties of the welded samples were investigated by changing the ratios of rotational speed (800−1200 r/min) to travel speed (40−100 mm/min) (ω/v). It was revealed that the grain growth rate was strongly increased with the increase of the heat input by rotational speed at constant travel speed, while the grain growth rate was slightly increased with the increase of the heat input by travel speed at constant rotational speed. Subsequently, hardness reduction was observed in the stir zone at higher rotational speed compared with that at lower one. An interesting observation was that various welding parameters do not have noticeable effect on the tensile strength of the FSW joints. Also, it has been observed that the fracture location of tensile test specimens was placed in the heat-affected zone (HAZ) on the advancing side at lower travel speed, while at higher travel speed, it was placed at the HAZ/thermomechanical affected zone (TMAZ) interface on the retreating side.

Key words: AA3003-H18 alloy; friction stir welding; heat input; microstructure; mechanical properties

1 Introduction

The most important process for the joining of aluminum alloys was the friction stir welding (FSW) that was developed within the last decade of the twentieth century as a solid-state joining technique at TWI in the UK in 1991 [1, 2]. FSW was initially applied to aluminum alloys and later, it was used for the welding of a wide variety of metallic materials such as copper and steel [3,4]. However, this process has been carried out on aluminum more than other metals and consequently, many researches have been done on this topic. Previous studies showed that during FSW of wrought aluminum alloys, the strength and hardness of the weld area were significantly reduced compared with those of base metal [3−7]. It is due to the high heat generation caused by friction and severe plastic deformation during FSW process [4,8,9]. Heat input of this welding process causes an annealing heat treatment in the weld area such as heat-affected zone (HAZ), thermomechanical affected zone (TMAZ) and stir zone (SZ). Phenomena that occur during annealing of these alloys include recovery and recrystallization [3,4,10,11]. Both of these phenomena eliminate the effects of strain hardening in the weld area and the dislocation density is reduced in the stir zone, HAZ and TMAZ of the friction stir welds compared with that in the base material [10,12,13]. Studies have shown that the reduction of dislocation density leads to the decrease of hardness and tensile strength in the weld region [14, 15]. Unlike non-heat-treatable alloys, the mechanical properties of heat-treatable aluminum alloys can be changed with time since they can be naturally age-hardened after friction stir welding [10,14,16]. In this class of alloys, FSW initially decreases the hardness of the stir zone in comparison with that of the base material. The strength and hardness of the weld zone regions can be improved with time due to the natural ageing of the material [14, 17]. But the mechanical properties of non-heat-treatable alloys are not changed with time after FSW, because they are non-precipitation-hardening. Therefore, it can be mentioned that, friction stir welding of wrought non-heat-treatable aluminum alloys has an adverse effect on their mechanical properties such as hardness and tensile strength caused by the heat input in weld regions (HAZ, TMAZ and stir zone) [3−5].

According to the above analyses, the heat input causes annealing and leads to a drop in hardness and strength in these materials. In this case the, reduction of

Corresponding author: M. KAZEMINEZHAD; Tel: +98-21-66165227, Fax: +98-21-66005717; E-mail: mkazemi@sharif.edu
DOI: 10.1016/S1003-6326(15)63826-2

mechanical properties in the weld zone can be avoided by controlling of heat input during FSW. One of the effective methods that have been proposed to control and minimize the heat input is the reduction of the ratio of rotational speed to travel speed (ω/v) or use of higher travel speeds and/or lower rotation speeds, because there is a direct correlation between the heat input and ω/v ratio [3,18−20]. The lower heat input can be achieved by decreasing the rotational speed (ω) and increasing the travel speed (v) [13,20]. On the other hand, the heat input is necessary to create a sound friction stir weld and this value cannot be too small; because the possibility of microstructural defects is increased due to insufficient heat input for appropriate material flow in stir zone [21−23]. Thus, it should be an optimal value.

The commercial 3003 (Al−Mn series) aluminum alloy is widely used in the container, automotive heat exchangers, packaging, and automobile industry due to its higher strength, corrosion resistance and formability [24−28]. This alloy is not heat-treatable, generally, and it is well known that the only way to improve the strength of such alloys is strain hardening through cold working [4,26]. Friction stir welding of as-received AA3003-H18 plate leads to reduction in hardness and strength of the weld zone due to the heat input of FSW. In 3003 aluminum alloy, the phenomenon of grain growth during heat treatment is severe compared with others and it is undesirable for mechanical properties [29]. Therefore, control of heat input in the major applications is very important in FSW of AA3003-H18 plate and efforts to achieve the optimum rotational and travel speeds and/or the optimum ratio of rotational speed to travel speed (ω/v) are necessary.

In the present work, 3 mm thick AA3003-H18 plates were used as the base material. The as-received plates were FSWed at the various rotational and travel speeds. The mechanical properties and microstructures of FSWed specimens were investigated and the influences of different rotational and travel speeds (or different ω/v values) were discussed.

2 Experimental

The initial materials were as-received AA3003-H18 plate with dimensions of 100 mm × 50 mm × 3 mm. The chemical composition of the alloy is shown in Table 1.

Table 1 Chemical composition of AA3003-H18 sheet (mass fraction, %)

Cu	Si	Fe	Mn	Al
0.065	0.222	0.353	0.944	Bal.

The welding tool was machined from H13 tool-steel and heat-treated to have hardness of HRC 50. A tool with a shoulder diameter of 20 mm was used to produce all of the welds discussed here and also the probe had a diameter of 5 mm and a height of 2.8 mm. The angle of tool tilt with respect to the workpiece surface was 2.5° from the vertical axis in the weld. The rotation speed range was from 800 to 1200 r/min and the traveling speed range was from 40 to 100 mm/min. The specimens were constrained by fixture during FSW process to prevent their movement.

In order to investigate the mechanical behavior of FSWed specimens, transverse tensile and microhardness profiles tests were carried out. The transverse tensile test specimens were prepared according to the ASTM-E8M standard that the stir zone was located in the center of gage length. The specimens for tensile test were prepared by cutting perpendicular to the welding direction. The microhardness of the centerline of the cross-section at a depth of 1.5 mm from the surface was measured using Vickers microhardness equipment with a load of 100 g for 15 s. The schematic diagram of FSW process and the position of microhardness and transverse tensile tests are shown in Figs. 1 and 2, respectively.

The microstructure was observed after polishing and electroetching by 3 mL HBF_4 + 100 mL distilled

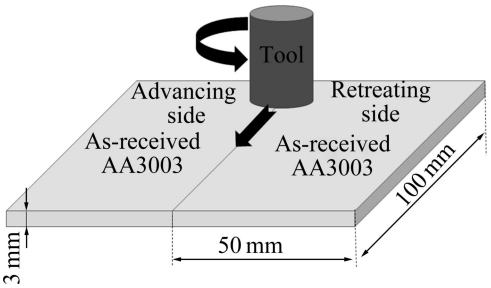

Fig. 1 Schematic illustration of FSW process

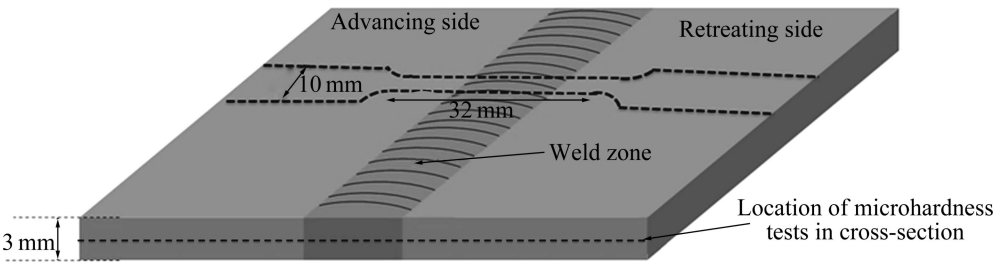

Fig. 2 Schematic diagram of transverse tensile and microhardness tests position

water at voltage of 20 V for 60 s. The microstructures of various regions of the joints were observed by optical microscopy (OM).

3 Results and discussion

3.1 Microstructure

Visual examination of the welded joints at various rotational and travel speeds show that the weld surface is dramatically influenced by rotational speed to travel speed (ω/v) ratio. The increase of ω/v value considerably makes a smooth and defect free weld on the surface. The large welding heat input due to high ω/v can cause a decent material flow throughout of the weld area. Therefore, increasing the speeds ratios (ω/v), from 8 to 30, makes a welding with high quality and good weld surface.

The cross-sections of the welded joints under various welding parameters were observed. Neither cracks nor porosity were visible, indicating a good quality of the joints. The optical microscope images of stir zone at various welding parameters are shown in Fig. 3. Microstructures show fine equiaxed grains under every FSW conditions in the stir zone. As can be seen in Fig. 3, the grain size in the stir zone increases with increasing the rotational speed at a constant travel speed. At higher rotational speed, the heat input is greater, due to the correlation between heat input and ω/v ratio that was described in the literature. Thus, with increasing ω/v ratio by the rotational speed, the heat input is increased and subsequently, the grain growth strongly occurs after recrystallization. Similar results have been obtained for FSW of aluminum alloys by other researchers [13,30,31].

According to the correlation between ω/v and heat input, the heat input is lower at higher travel speed. It is expected that the smaller grain size is achieved with increasing the travel speed in the stir zone of welds. But it can hardly be seen in Fig. 3. According to Figs. 3 (a)−(c), (d)−(f) and (g)−(i) with rotational speeds at 800 r/min, 1000 r/min and 1200 r/min, respectively, with increasing the travel speed from 40 mm/min to 100 mm/min, the grain size is slightly changed. The average grain size of the stir zone provided in Table 2 confirms this statement. Also, Fig. 4 shows the variations of grain size of the stir zone versus the rotational speed. It should be noted that all images in Fig. 4 are taken from the advancing side of joints at a depth of 1.5 mm and a distance of 12 mm from the weld center. As can be seen, the grain size range varies (7.8−22 μm) with the rotational speed and the smallest and largest grain size is related to specimens with the lowest and highest ω/v, respectively. It is clearly understood from Fig. 4 that decreasing travel speed has little effect on the grain growth. In fact, the increase in travel speed leads to the fast moving heat source and heat generation because

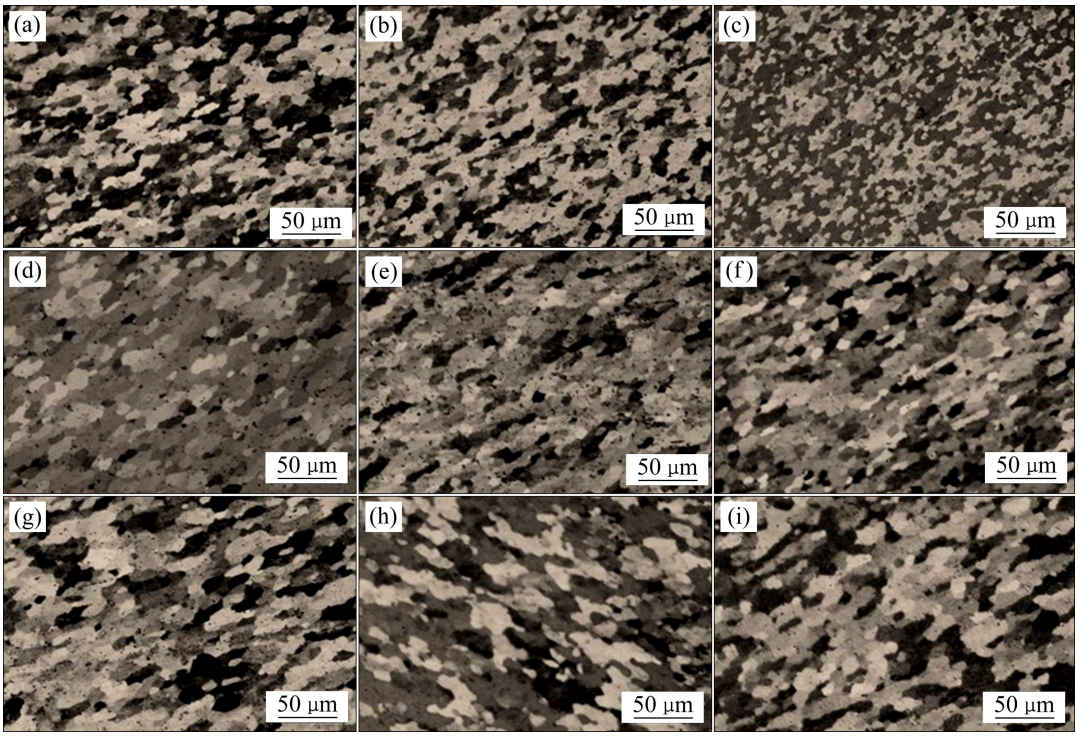

Fig. 3 Optical microscope images of stir zone at different rotational (ω) and travel speeds (v): (a) 800 r/min, 40 mm/min; (b) 800 r/min, 70 mm/min; (c) 800 r/min, 100 mm/min; (d) 1000 r/min, 40 mm/min; (e) 1000 r/min, 70 mm/min; (f) 1000 r/min, 100 mm/min; (g) 1200 r/min, 40 mm/min; (h) 1200 r/min, 70 mm/min; (i) 1200 r/min, 100 mm/min

Table 2 Average grain size values of stir zone welded at various welding parameters

Rotational speed/(r·min^{-1})	Average grain size/μm		
	40 mm/min	70 mm/min	100 mm/min
800	13.6	13.6	7.8
1000	16.7	16	15.8
1200	22	20.7	21

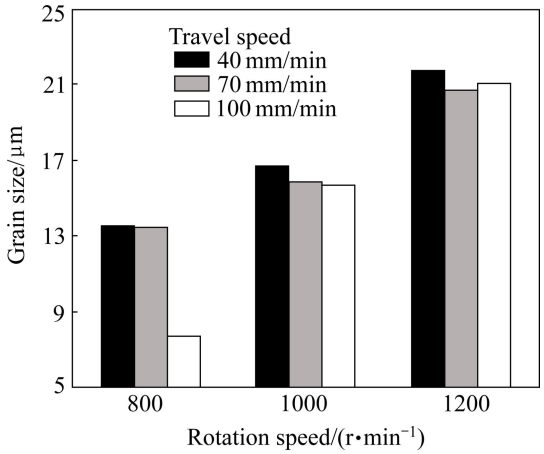

Fig. 4 Effect of rotational speed on grain size of stir zone

friction and deformation have relatively less retention time to conduct around. Consequently, the heat is not focused in the stir zone and grain growth occurs slightly.

The microstructure images of HAZ at various welding parameters are shown in Fig. 5. Comparison of Fig. 3 with Fig. 5 indicates that all the stir zones clearly show finer grains than the heat-affected zones. It is due to severe plastic deformation and high temperature, leading to dynamic recrystallization. The relationship between microstructure of the HAZ and welding parameters (heat input or ω/v value) is strongly similar to those in the stir zone. The average grain size of the HAZ given in Table 3 confirms this statement and its range is from 20.4 μm to 41.7 μm. Also, Fig. 6 shows the variations of grain size in the HAZ as a function of rotational speed. According to these experimental results, it can be said that the grain size is influenced by the rotational speed and the reduction of travel speed has no effect on grain growth.

3.2 Mechanical properties

The mechanical properties of the base metal are shown in Table 4. Tensile properties of friction stir welded joints were measured by performing tensile tests on transverse tensile samples containing weld zone at the center. Figure 7 shows the stress−strain curves for base material (Fig. 7(a)) and friction stir welded joints at various welding parameters. The results of the tensile tests are shown in Table 5. These results include tensile strength and fracture locations of the joints under tension

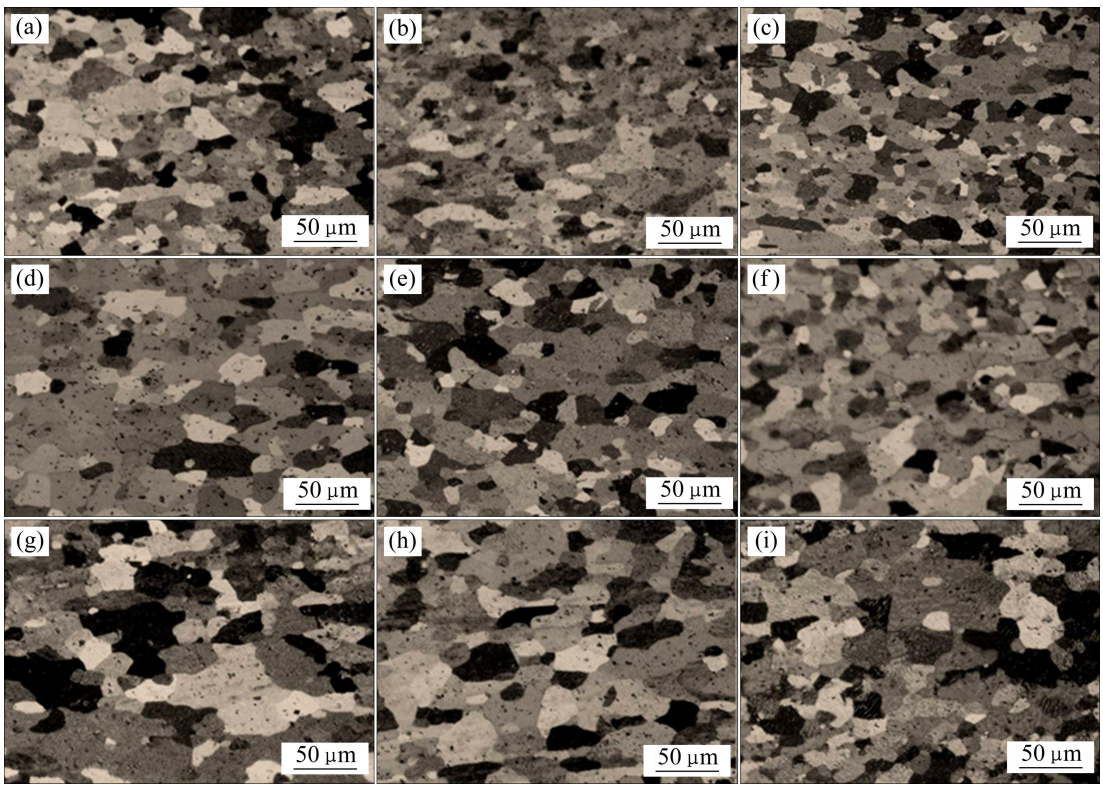

Fig. 5 Optical microscope images of HAZ at various rotational (ω) and travel speeds (v): (a) 800 r/min, 40 mm/min; (b) 800 r/min, 70 mm/min; (c) 800 r/min, 100 mm/min; (d) 1000 r/min, 40 mm/min; (e) 1000 r/min, 70 mm/min; (f) 1000 r/min, 100 mm/min; (g) 1200 r/min, 40 mm/min; (h) 1200 r/min, 70 mm/min; (i) 1200 r/min, 100 mm/min

Table 3 Average grain size values of HAZ at various welding parameters

Rotational speed/(r·min^{-1})	Average grain size/μm		
	40 mm/min	70 mm/min	100 mm/min
800	23.0	22.8	20.4
1000	33.3	26.3	28.7
1200	41.7	36.6	26.5

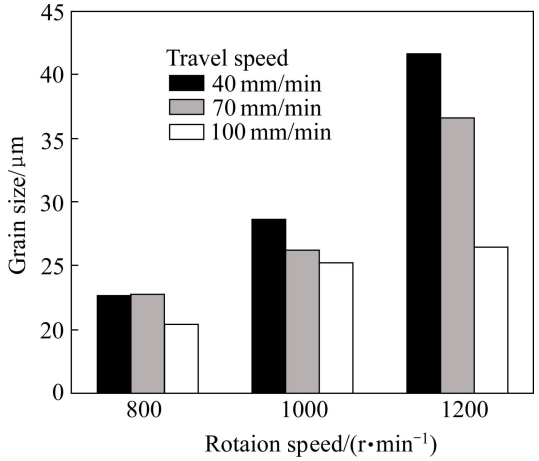

Fig. 6 Effect of rotational speed on grain size of heat-affected zone

Table 4 Mechanical properties of wrought base metal (AA3003-H18)

Tensile strength/MPa	Hardness (HV)	Elongation/%
202	47	4.7

with various welding parameters. As can be seen in Figs. 7(b)−(d), the welding parameters do not have noticeable effect on the tensile strength of the FSW joints. In other words, there is not much difference between the values obtained for tensile strength of specimens and these are very insensitive to the welding parameters. Differences are very slight and cannot be considered conclusive. One of the previous work [4] described that the tensile strength values of non-heat-treatable alloys are relatively insensitive to the welding parameters (so long as no weld defects are generated). According to Fig. 7, large increase in tensile elongation of the welded specimens is observed in comparison with that of base metal due to annealing or thermal softening [3,4]. At low travel speed, high heat generation causes higher annealing temperature and increases the elongation [31]. This is the reason for the increase in elongation, as shown in Fig. 8.

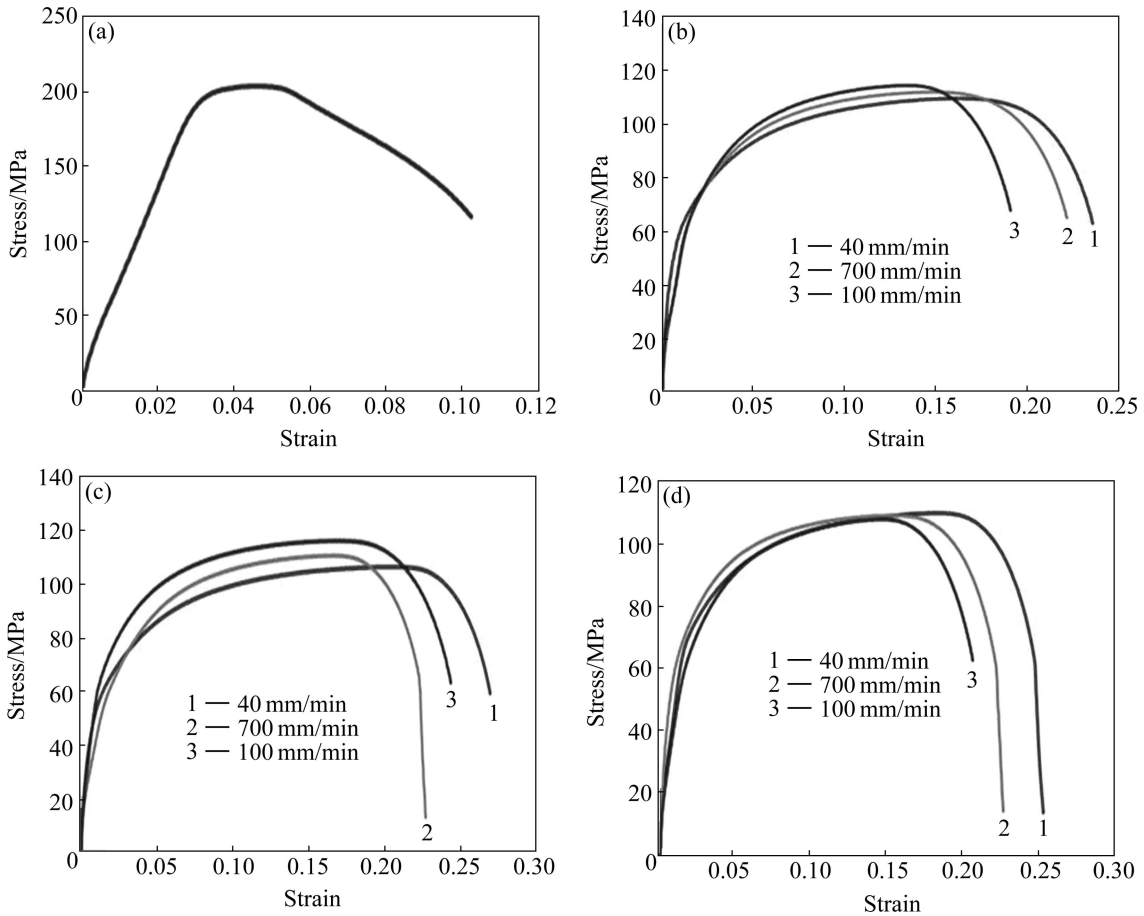

Fig. 7 Stress−strain curves of tensile specimens for base metal (a) and friction stir welded joints of AA3003-H18 at various traveling speeds with constant rotational speed of 800 r/min (b), 1000 r/min (c) and 1200 r/min (d)

Table 5 Summary of tensile test results of specimens after FSW

Rotational speed/ ($r \cdot min^{-1}$)	Travel speed/ ($mm \cdot min^{-1}$)	Tensile strength/MPa	Fracture locations of joints
800	40	109.7	HAZ
800	70	112	HAZ/TMAZ interface
800	100	114.4	HAZ/TMAZ interface
1000	40	107	HAZ
1000	70	111	HAZ
1000	100	116	HAZ/TMAZ interface
1200	40	110.2	HAZ
1200	70	109.4	HAZ
1200	100	108	HAZ/TMAZ interface

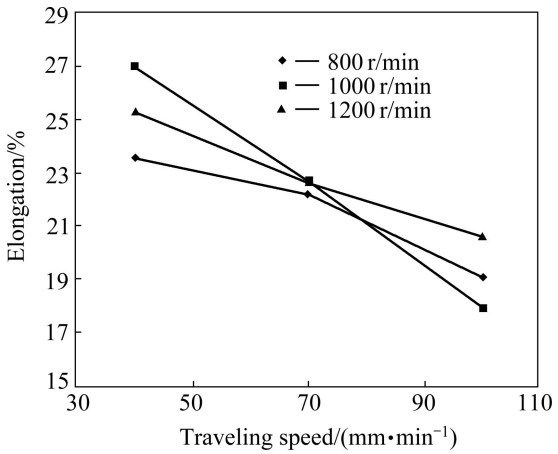

Fig. 8 Effect of traveling speed on elongation

In general, the fracture of defect-free sound welded joints during tensile test takes place from minimum hardness region [31]. It is revealed that the fracture location of welds under tension tests depends on the welding parameters (Fig. 9). As can be seen in Fig. 9, generally, increase in heat input due to decreasing travel speed makes the samples fracture at HAZ/TMAZ interface (within weld zone). So that in all cases with low travel speed (40 mm/min), the fracture location under tensile test is placed in the HAZ. While, in all cases with high travel speed (100 mm/min), it is placed within weld zone or at HAZ/TMAZ interface. As mentioned in Section 3.1, the amount of heat supplied to the deforming material in weld area is greater at lower travel speed (high ω/v value); thus wider areas are affected by the heat input and softened [31]. As a result, the wider area is annealed, leading to thermal softening and loss of strength. Close results were reported by SHARMA et al [31] about fracture locations.

Another issue that is clearly observed in Fig. 9 is the dependence of the failure side on welding parameters. In samples with low travel speed (high heat input), the failure side is placed on the advancing side, while in samples with high travel speed (low heat input), the failure side is placed on the retreating side and within weld zone. It can be explained by considering the sources of heat generation in FSW process. Generally, heat generation takes place in two ways in FSW: one is the friction between the rotational tool and the workpiece, and the other is plastic deformation. Both of them occur during FSW process. It has been reported that the heat generation caused by friction is higher on the advancing side compared with the retreating side, because of the same direction of rotational and travel speed on the advancing side [5,13]. On the other hand, the heat generation caused by the plastic strain is higher on the retreating side compared with that on the advancing side. It can be attributed to the asymmetrical distribution of plastic strains, because the severe plastic deformation is much smaller on the advancing side than that on the retreating side [31−34]. According to the above-mentioned results, in samples with lower travel speed, heat generation caused by friction is probably more than that generated by plastic deformation. As a result, grain growth and thermal softening in the HAZ on the advancing side is more than that on the retreating side one, corresponding to fracture locations in the HAZ on the advancing. But in samples with higher travel speed,

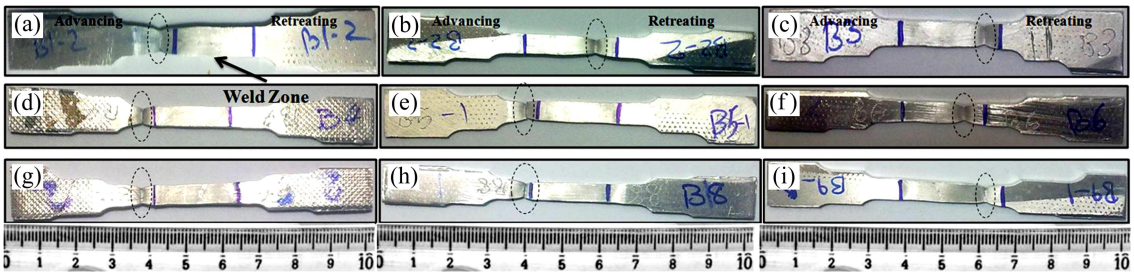

Fig. 9 Macro images of fractured transverse tensile specimens after FSW process at various rotational (ω) and travel speeds (v): (a) 800 r/ min, 40 mm/min; (b) 800 r/mim, 70 mm/min; (c) 800 r/min, 100 mm/min; (d) 1000 r/min, 40 mm/min; (e) 1000 r/min, 70 mm/min; (f) 1000 r/min, 100 mm/min; (g) 1200 r/min, 40 mm/min; (h) 1200 r/min, 70 mm/min; (i) 1200 r/min, 100 mm/min

heating due to the plastic strain is probably dominated, thus it leads to fracture in the weld zone on the retreating side.

Figure 10 shows the hardness distribution in the cross-section (in depth of 1.5 mm) of the welded specimens with different parameters. As it is expected, the hardness has reduction in different regions of the weld (stir zone, TMAZ and HAZ) compared with that of the base metal, which is 42% (HV 27), depending on welding parameters. As can be seen in Fig. 10, the hardness values in the stir zone are identical at various travel speeds and constant rotational speed (800, 1000 and 1200 r/min). This is consistent with the results of the microstructure that is mentioned in Fig. 3.

According to Fig. 10, widening of HAZ at low travel speed is quite evident. For example, it can be seen in Fig. 10(a) that with increasing the heat input due to the decreasing of travel speed, the extent of area with low hardness (or HAZ) is dramatically increased. So, with decreasing the travel speed from 100 mm/min to 40 mm/min, the HAZ is almost doubled. In Fig. 11, the effect of rotational speed on the hardness values in the stir zone and HAZ is shown. Each point of the curve is the average of six points of hardness. As can be seen, in both zones, the hardness is reduced with increasing rotational speed and constant travel speed. This can be attributed to the grain growth at high rotational speeds or high ω/v value (see Figs. 3 and 5).

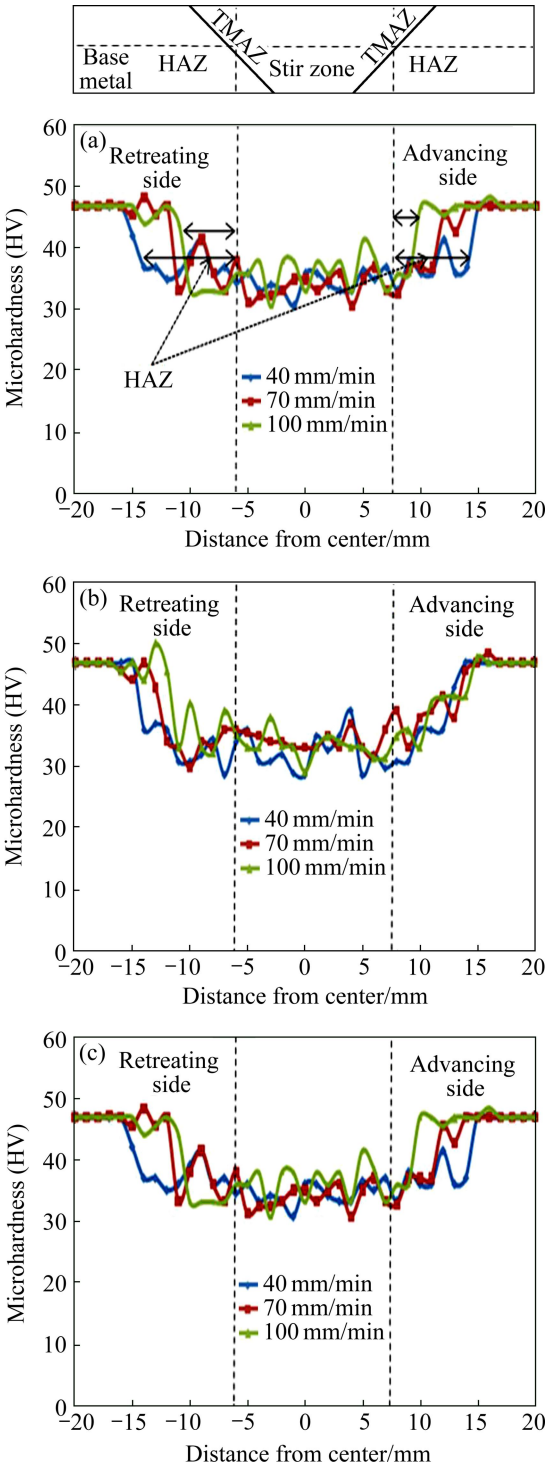

Fig. 10 Hardness distributions in cross-section after FSW at different rotational speeds: (a) 800 r/min; (b) 1000 r/min; (c) 1200 r/min

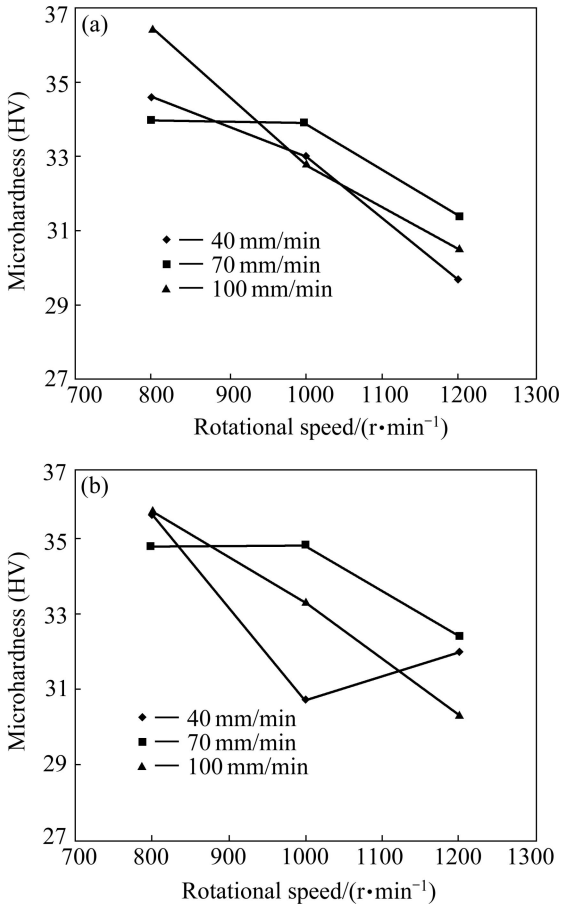

Fig. 11 Microhardness variations as function of rotational speeds in stir zone (a) and HAZ (b)

4 Conclusions

1) The average grain size increases with increasing the heat input (or ω/v value) in both the stir zone and

HAZ. But the grain growth is mainly influenced by increasing of rotational speed and decreasing of travel speed.

2) It is found from the fracture locations of tensile test specimens and microhardness measurements that the HAZ becomes wider with decreasing of travel speed.

3) The fracture locations and side of fracture are strongly dependent on the welding parameters, so that it is placed in the HAZ on the advancing side at low travel speed and in the HAZ/TMAZ interface on the retreating side at high travel speed.

4) The results show that the decreasing of traveling speed (or increase the heat input) in constant rotational speed increases the elongation of welded specimens. Also, the tensile strength values are insensitive to the welding parameters (ω and v).

5) Increase in rotation speed reduces the hardness in the stir zone, while the change of travel speed does not have a substantial effect on the hardness of stir zone.

Acknowledgments

The authors wish to thank the research board of Sharif University of Technology for the financial support and the provision of the research facilities used in this work.

References

[1] MATHERS G. The welding of aluminium and its alloys [M]. Cambridge, England: Woodhead Publishing Limited, 2002: 161.

[2] NANDAN R, DEBROY T, BHADESHIA H K D H. Recent advances in friction-stir welding–process [J]. Weldment Structure and Properties, Progress in Materials Science, 2008, 53(6): 980−1023.

[3] THREADGILL P L, LEONARD A J, SHERCLIFF H R, WITHERS P J. Friction stir welding of aluminium alloys [J]. International Materials Reviews, 2009, 54(13−14): 49−93.

[4] MISHRA R S, MAHONEY M W. Friction stir welding and processing [M]. ASM International, 2007.

[5] MISHRA R S, MA Z Y. Friction stir welding and processing [J]. Materials Science and Engineering R, 2005, 50: 1−78.

[6] LIU H J, FUJII H, NOGI K. Tensile properties of a friction stir welded thin-sheet of 1050-H24 aluminum alloy [J]. Characterization & Control of Interfaces for High Quality Advanced Materials, 2006, 146: 129−136.

[7] PEEL M, STEUWER A, PREUSS M, WITHERS P J. Microstructure, mechanical properties and residual stresses as a function of welding speed in aluminium AA5083 friction stir welds [J]. Acta Materialia, 2003, 51(16): 4791−4801.

[8] ĐURĐANOVIĆ M B, MIJAJLOVIĆ M M, MILČIĆ D S, STAMENKOVIĆ D S. Heat generation during friction stir welding process [J]. Tribology in Industry, 2009, 31: 8−14.

[9] SCHMIDT H, HATTEL J, WERT J. An analytical model for the heat generation in friction stir welding [J]. Modelling and Simulation in Materials Science and Engineering, 2004, 12: 143−157.

[10] WOO W, BALOGH L, UNGÁR T, CHOO H, FENG Z. Grain structure and dislocation density measurements in a friction-stir welded aluminum alloy using X-ray peak profile analysis [J]. Materials Science and Engineering A, 2008, 498(1−2): 308−313.

[11] XU W F, LIU J H, CHEN D L, LUAN G H, YAO J S. Improvements of strength and ductility in aluminum alloy joints via rapid cooling during friction stir welding [J]. Materials Science and Engineering A, 2012, 548: 89−98.

[12] SARKARI KHORRAMI M, KAZEMINEZHAD M, KOKABI A H. Thermal stability during annealing of friction stir welded aluminum sheet produced by constrained groove pressing [J]. Materials & Design, 2013, 45: 222−227.

[13] SARKARI KHORRAMI M, KAZEMINEZHAD M, KOKABI A H. Microstructure evolutions after friction stir welding of severely deformed aluminum sheets [J]. Materials & Design, 2012, 40: 364−372.

[14] LINTON V M, RIPLEY M I. Influence of time on residual stresses in friction stir welds in agehardenable 7xxx aluminium alloys [J]. Acta Materialia, 2008, 56(16): 4319−4327.

[15] YADAV D, BAURI R. Effect of friction stir processing on microstructure and mechanical properties of aluminium [J]. Materials Science and Engineering A, 2012, 539: 85−92.

[16] FRIGAARD Ø, GRONG Ø, MIDLING O T. A process model for friction stir welding of age hardening aluminum alloys [J]. Metallurgical and Materials Transactions A, 2011, 32(5): 1189−1200.

[17] FU R D, ZHANG J F, LI Y J, KANG J, LIU H J, ZHANG F C. Effect of welding heat input and post-welding natural aging on hardness of stir zone for friction stir-welded 2024-T3 aluminum alloy thin-sheet [J]. Materials Science and Engineering A, 2013, 559: 319−324.

[18] KUMAR R, SINGH K, PANDEY S. Process forces and heat input as function of process parameters in AA5083 friction stir welds [J]. Transactions of Nonferrous Metals Society of China, 2012, 22(2): 288−298.

[19] DEHGHANI M, MOUSAVI S A A A, AMADEH A. Effects of welding parameters and tool geometry on properties of 3003-H18 aluminum alloy to mild steel friction stir weld [J]. Transactions of Nonferrous Metals Society of China, 2013, 23(7): 1957−1965.

[20] KHORRAMI M S, KAZEMINEZHAD M, KOKABI A H. Mechanical properties of severely plastic deformed aluminum sheets joined by friction stir welding [J]. Materials Science and Engineering A, 2012, 543: 243−248.

[21] POPOVIĆ O, PROKIĆ-CVETKOVIĆ R, BURZIĆ M, MILUTINOVIĆ Z. The effect of heat input on the weld metal toughness of surface welded joint [C]// Proceedings of the 14th International Research/Expert Conference. Mediterranean Cruise, 2010: 61−64.

[22] MOVAHEDI M, KOKABI A H, REIHANI S M S, NAJAFI H. Effect of tool travel and rotation speeds on weld zone defects and joint strength of aluminium steel lap joints made by friction stir welding [J]. Science and Technology of Welding and Joining, 2012, 17: 162−167.

[23] ABBASI GHARACHEH M, KOKABI A H, DANESHI G H, SHALCHI B, SARRAFI R. The influence of the ratio of rotational speed/traverse speed (ω/V) on mechanical properties of AZ31 friction stir welds [J]. International Journal of Machine Tools and Manufacture, 2006, 46(15): 1983−1987.

[24] AYDIN H, BAYRAM A, YILDIRIM M T, YIĞIT K. Influence of welding parameters on the fatigue behaviours of friction stir welds of 3003-O aluminum alloys [J]. Materials Science, 2010, 16(4): 311−319.

[25] BOZKURT Y, DUMAN S. The effect of welding parameters on the mechanical and microstructural properties of friction stir welded dissimilar AA 3003-H24 and 2124/SiC/25p−T4 alloy joints [J]. Scientific Research and Essays, 2011, 6: 3702−3716.

[26] KAUFMAN J G. Introduction to aluminum alloys and tempers [M].

Materials Park: ASM International, 2000.
[27] JARADEH M M R, CARLBERG T. Solidification studies of 3003 aluminium alloys with Cu and Zr additions [J]. Journal of Materials Science & Technology, 2011, 27(7): 615−627.
[28] HUANG H W, OU B L. Evolution of precipitation during different homogenization treatments in a 3003 aluminum alloy [J]. Materials & Design, 2009, 30(7): 2685−2692.
[29] TOTTEN G E. Handbook of aluminum (alloy production and materials manufacturing) [M]. Vol. 2. New York: Marceld Dekker, Inc, 2003.
[30] HIRATA T, OGURI T, HAGINO H, TANAKA T, CHUNG S W, TAKIGAWA Y. Influence of friction stir welding parameters on grain size and formability in 5083 aluminum alloy [J]. Materials Science and Engineering A, 2007, 456(1−2): 344−349.
[31] SHARMA C, DWIVEDI D K, KUMAR P. Effect of welding parameters on microstructure and mechanical properties of friction stir welded joints of AA7039 aluminum alloy [J]. Materials & Design, 2012, 36: 79−390.
[32] SHARMA D, BHUSHAN R K. Thermomechanical modeling of FSW: A review [J]. International Journal of Emerging Technology and Advanced Engineering, 2013, 3(2): 130−135.
[33] REYNOLDS A, LOCKWOOD W, SEIDEL T. Processing-property correlation in friction stir welds [J]. Materials Science Forum, 2000, 331−337: 1719−1724.
[34] ZHANG Z, LIU Y L, CHEN J T. Effect of shoulder size on the temperature rise and the material deformation in friction stir welding [J]. The International Journal of Advanced Manufacturing Technology, 2009, 45(9−10): 889−895.

热输入对搅拌摩擦焊 AA3003-H18 板材显微组织和力学性能的影响

B. ABNAR, M. KAZEMINEZHAD, A. H. KOKABI

Department of Materials Science and Engineering, Sharif University of Technology, Azadi Avenue, Tehran, Iran

摘　要：通过优化焊接参数，采用搅拌摩擦焊对不可热处理强化 A3003-H18 合金进行焊接以获得合适的接头。通过改变转速(800~1200 r/min)和行进速度(40~100 mm/min)比(ω/v)，研究热输入对焊接样品显微组织和力学性能的影响。结果表明，随着转速提高，热输入增加，晶粒增长速度大幅增加，而随着行进速度提高，热输入增加，但晶粒增长速度略有增加。与低转速相比，高转速会降低搅拌区的硬度。而不同焊接参数对接头的拉伸强度的影响不明显。在低行进速度时，拉伸样品的断裂位置在前进侧的热影响区(HAZ)；而在高行进速度时，断裂位置在后退侧的 HAZ/TMAZ 界面。

关键词：AA3003-H18 合金；搅拌摩擦焊；热输入；显微组织；力学性能

(Edited by Yun-bin HE)